Semiclassical Eigenvalue Distribution of the Non Self-Adjoint Zakharov-Shabat Eigenvalue Problem.

Jared C. Bronski
Institute for Math. and its Applications *
University of Minnesota
Minneapolis, MN 55455.

1 March 1995

Abstract

ABSTRACT: In this paper we review the theory of the semiclassical limit of the non self-adjoint Zakharov-Shabat eigenvalue problem. We conduct a series of careful numerical experiments which provide strong evidence that the number of eigenvalues scales like ϵ^{-1}, just as in the self-adjoint case, and that the eigenvalues appear to approach a limiting curve. One general choice of potential functions produces a 'Y' shaped spectrum. We give an asymptotic argument which predicts a critical value for the phase for which the straight line spectra bifurcates to produce the 'Y' shaped spectra. We also show that the number of eigenvalues living away from the real axis for a restricted class of potentials is bounded by $c\epsilon^{-1}$, where c is an explicit constant. A complete theory of the shape of the eigenvalue curve and a general bound on the number of eigenvalues is still lacking.

*Partially Supported by an NSF Postdoctoral Fellowship

1. Introduction

Since the earliest days of quantum mechanics it has been known that

$$\begin{aligned} i\epsilon\psi_t &= -\epsilon^2\psi_{xx} + V(x)\psi \\ \psi(x,0) &= A(x)\exp(iS(x)/\epsilon) \end{aligned}$$

provides the bridge bewteen classical and quantum mechanics. A formal expansion in powers of ϵ leads to the eikonal and transport equations

$$\begin{aligned} S_t &= S_x^2 + V(x) \\ A_t &= 2S_xA_x + S_{xx}A. \end{aligned}$$

The eikonal equation can be solved by the method of characteristics. The characteristic curves for the eikonal equation satisfy

$$\begin{aligned} \frac{dx}{dt} &= P \\ \frac{dP}{dt} &= -\nabla V, \end{aligned}$$

where $P = S_x$. These are the classical trajectories of the system in question. Thus the eikonal equation contains all of the classical mechanics of the system, and the semiclassical limit represents one order beyond the classical approximation.

It was first observed by Lax and Levermore[21] in a series of three papers in 1983 that a similar limit could be done in an exact way for the KdV equation

$$U_t = UU_x + \epsilon^2 U_{xxx}.$$

The KdV equation can be solved by the method of inverse scattering using the associated scattering problem

$$\lambda\phi = -\epsilon\phi_{xx} + U(x,0)\phi.$$

The solution of the above eigenvalue problem in the limit as $\epsilon \to 0$ is a classical problem in physics, with well known expressions available for the distribution of eigenvalues. Using this result on the distribution of the eigenvalues Lax and Levermore were able to show that the solutions of the slightly dispersive KdV equation,

$$U_t = UU_x + \epsilon^2 U_{xxx},$$

approached strongly the solution of the Hopf equation

$$U_t = UU_x$$

as $\epsilon \to 0$ as long as the solutions of the latter remained classical (i.e. before the development of the first shock.) After the time of first shock the solutions to the slightly dispersive KdV weakly approach a function which arises as the minima of a variational problem. The approach is weak because of the development of rapid oscillations which, nonetheless, have a well defined envelope.

Since the original work of Lax and Levermore on the dispersionless limit of the KdV equation there has been a small industry devoted to using the inverse scattering transform to explicitly calculate the evolution of nonlinear wave equations in the semi-classical limit. In particular this sort of calulation has been done for KdV, defocusing NLS, the Toda lattice[17, 18, 21, 28], etc. With few exceptions[10] the integrable systems for which this type of calculation has been done are associated with self-adjoint scattering problems, and possess well-posed (hyperbolic) modulation equations. For equations of the focusing NLS type, where the associated eigenvalue problem is not self-adjoint, the semiclassical distribution of eigenvalues is not at all understood. In particular it is not known how the number of eigenvalues scales with ϵ, the semiclassical parameter, and how these eigenvalues are distributed in the complex plane. In order to understand the semiclassical limit of equations like the focusing NLS, and observed phenomena like the 'sea of solitons', it is necessary to understand these sorts of properties of semi-classical limits of non self-adjoint eigenvalue problems. This is the problem we consider in this paper.

2. The Formal WKB Calculation.

In this section we review the formal WKB calculation as applied to the ZS eigenvalue problem (the calculation given here is modeled on one due to Deift[6]). This calculation is interesting because it motivates the introduction of the turning point curve, which appears to be important to understanding the semi-classical limit. Unfortunately, the exact significance of this object is not completely understood.

We are considering the semiclassical scaling of the non self-adjoint Zakharov-Shabat scattering problem,

$$i\epsilon v_x = qw + \lambda v \tag{2.1}$$

$$i\epsilon w_x = \bar{q}v - \lambda w, \tag{2.2}$$

subject to L_2 boundary conditions, where the potential function is of the form

$$q(x) = A(x)e^{iS(x)/\epsilon}.$$

Since the potential q is rapidly varying it is necessary to factor out the rapid variations in order to be able to apply WKB theory. Making the change of variables

$$\tilde{v} = ve^{-iS(x)/2\epsilon}$$

$$\tilde{w} = we^{iS(x)/2\epsilon},$$

leads to the following equations for $\tilde{v}, \tilde{w}$:

$$i\epsilon\tilde{v}_x = A\tilde{w} + (\lambda + S_x/2)\tilde{v} \tag{2.3}$$

$$i\epsilon\tilde{w}_x = A\tilde{v} - (\lambda + S_x/2)\tilde{w}, \tag{2.4}$$

or, in more compact notation

$$i\epsilon\vec{v}_x = \mathbb{M}(x,\lambda)\vec{v}.$$

At this point we make the assumption that the matrix $\mathbb{M}$ is diagonalizable, and introduce the normalized left and right eigenvectors $\vec{l}, \vec{r}$ and the associated eigenvalues μ_i:

$$\vec{l}_i(x,\lambda)\mathbb{M} = \mu_i(x,\lambda)\vec{l}_i(x,\lambda) \tag{2.5}$$

$$\mathbb{M}\vec{r}_i(x,\lambda) = \mu_i(x,\lambda)\vec{r}_i(x,\lambda) \tag{2.6}$$

$$\vec{l}_i \cdot \vec{r}_i = \delta_{i,j}. \tag{2.7}$$

We make the WKB ansatz

$$\vec{v} = e^{-i\phi(x,\lambda)/\epsilon}(\vec{v}^0 + \epsilon\vec{v}^1 + ..)$$

and collect powers of ϵ. The leading order (eikonal) equation is

$$O(1) \qquad \phi_x \vec{v}^0 = \mathbb{M}\vec{v}^0.$$

This implies that v^0 is an eigenvector of $\mathbb{M}$, and ϕ_x is the associated eigenvalue. Note that any scalar function of x multiplied by v^0 also satisfies the eikonal equation. Thus we can write

$$\vec{v}^0 = \alpha(x)\vec{r}_i,$$

where α is some undetermined function of x. This ambiguity will be settled as a solvability condition at the next order in perturbation theory.

The next order (transport) equation is

$$O(\epsilon) \qquad \phi_x \vec{v}^1 - \mathbb{M}\vec{v}^1 + \alpha_x \vec{r}_i + \alpha \vec{r}_{i,x} = 0.$$

We take the inner product of the above equation with the adjoint eigenvector $\vec{l}_i$ and apply the Fredholm alternative. This results in the transport equation

$$\alpha_x + \alpha \vec{l}_i \cdot \vec{r}_{i,x} = 0,$$

which can immediately be integrated to yield

$$\alpha = \alpha_o e^{-\int \vec{l}_i \cdot \vec{r}_{i,x}}.$$

Note that if $\mathbb{M}(x, \lambda)$ is an analytic matrix valued function of x and it is diagonalizable, as we assumed, then the left/right eigenvectors are differentiable. Also note that the arbitrary (x-independent) constant which arises is simply due to the linearity of the problem. Higher order terms can be calculated similarly.

For the Zakharov-Shabat eigenvalue problem the matrix $\mathbb{M}$ is given by

$$\mathbb{M} = \begin{pmatrix} \lambda - S_x/2 & A \\ A & S_x/2 - \lambda \end{pmatrix} = \begin{pmatrix} \alpha & \beta \\ \beta & -\alpha \end{pmatrix}$$

and the left and right eigenvectors are given by

$$\begin{aligned} \vec{l}_\pm &= \begin{pmatrix} \alpha \pm \sqrt{\alpha^2 + \beta^2} & \pm\beta \end{pmatrix} \\ \vec{r}_\pm &= \begin{pmatrix} \alpha \pm \sqrt{\alpha^2 + \beta^2} \\ \pm\beta \end{pmatrix}. \end{aligned}$$

The corresponding amplitude function is given by

$$A(x) = \sqrt{\alpha^2 + \beta^2 \pm \alpha\sqrt{\alpha^2+\beta^2}},$$

which means that to within the physical optics approximation the solutions are given by

$$\vec{v} \approx \begin{pmatrix} (1 \pm \frac{\alpha}{\sqrt{\alpha^2+\beta^2}})^{1/2} \\ \frac{\beta}{(\alpha^2+\beta^2)^{1/4}(\alpha\pm(\alpha^2+\beta^2)^{1/2})^{1/2}} \end{pmatrix} \exp(\pm i \int \sqrt{\alpha^2+\beta^2}).$$

3. The Breakdown of WKB - Turning Points.

The phase function $\phi_x^{\pm}(x,\lambda)$ is given by the eigenvalues of the matrix

$$\mathbb{M}(x,\lambda) = \begin{pmatrix} (\lambda + S_x/2) & A \\ A & -(\lambda + S_x/2) \end{pmatrix}.$$

Specifically

$$\phi_x^{\pm} = \pm\sqrt{(\lambda + S_x/2)^2 + A^2}.$$

The above analysis assumed that $\mathbb{M}(x,\lambda)$ is diagonalizable. This is true, since the eigenvalues are distinct, except when $\phi_x^{\pm} = 0$, when $\mathbb{M}$ is nilpotent and thus NOT diagonalizable. This occurs when

$$\begin{aligned} \phi_x = 0 \qquad &=> \quad (\lambda - S_x/2)^2 + A^2 = 0 \\ &=> \quad \lambda = S_x/2 \pm i|A|. \end{aligned}$$

Thus if λ lies on the curve $\Gamma = \{S_x/2 \pm i|A| \big| x \in (-\infty,\infty)\}$ then the WKB solution breaks down at some point, otherwise it is well behaved for all x. We refer to Γ as the turning point curve.

Since we are interested in L_2 solutions it is important to understand the asymptotics of the WKB solutions. The controlling behavior of $\vec{v}_{WKB}$ at $x = \pm\infty$ is governed by the phase function ϕ_x. As $x \to \pm\infty$ the phase function $\phi_x \to \pm\lambda$. The important thing to realize is that the limiting values of ϕ_x at $\pm\infty$ *needn't be the same*. In other words there are two possible scenarios: ($\phi^- = -\phi^+$):

Case 1: (The 'homoclinic' case)

$$\phi_x^+ \to \begin{cases} \lambda & \text{as } x \to -\infty \\ \lambda & \text{as } x \to +\infty. \end{cases}$$

Case 2: (The 'heteroclinic' case)

$$\phi_x^+ \rightarrow \begin{cases} -\lambda & \text{as} \quad x \rightarrow -\infty \\ \lambda & \text{as} \quad x \rightarrow +\infty. \end{cases}$$

Assuming λ does not lie on the turning point curve Γ, so that the WKB expansion does not break down for finite x, we need to determine for which values of λ the phase function ϕ_x is in the "heteroclinic" case, and for which λ the phase function is in the "homoclinic" case. If λ is in the heteroclinic case then for large x one WKB solution behaves like $\exp(\lambda_{imag}|x|)$, , while the other behaves like $\exp(-\lambda_{imag}|x|)$. On the other hand if λ is in the homoclinic case then when x is large one WKB solution behaves like $\exp(\lambda_{imag}x)$, while the other behaves like $\exp(-\lambda_{imag}x)$. Thus to within the WKB approximation any λ in the heteroclinic case appears to represent an eigenvalue, while no λ in the homoclinic case represents an eigenvalue!

The problem of determining which λ are in the heteroclinic case and which λ are in the homoclinic case turns out to be quite trivial. In the case $S_x, A \rightarrow 0$ as $|x| \rightarrow \infty$, for example, the set of λ which are in the heteroclinic case is exactly the interior of the discriminant curve Γ. This is illustrated in figures 3.1,3.2,3.3, where we have chosen the amplitude and phase functions to be given by

$$\begin{aligned} S(x) &= \operatorname{sech}(x) \\ A(x) &= \operatorname{sech}(x). \end{aligned}$$

The figure 3.1 shows the discriminant curve, along with a typical interior point and a typical exterior point. Figures 3.2, 3.3 show the real and imaginary parts of the phase function ϕ_x for λ in the interior and exterior regions respectively.

3.1. The WKB 'Paradox'

Having done the WKB analysis, we arrive at the apparent paradox - any λ which lies on the interior of the turning point curve Γ appears to be an eigenvalue. This clearly cannot be right. So what goes wrong with WKB theory?

This paradox is not new to the ZS problem. It is the same phenomenon which arises in the WKB theory for the Schrödinger equation, where it is commonly known as the "WKB paradox". In

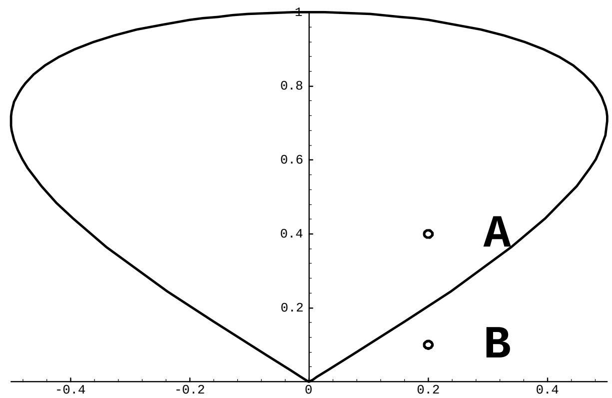

Figure 3.1: The Turning Point Curve

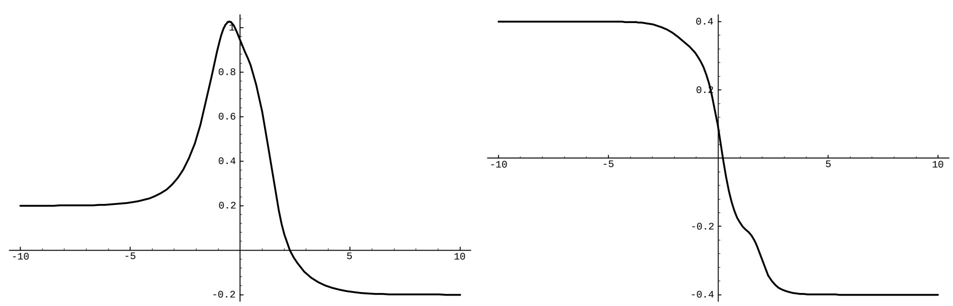

(a) Real Part

(b) Imaginary Part

Figure 3.2: The Phase Function - Heteroclinic Case - A

the context of the Schrödinger equation it takes the following form. Consider the Schrödinger equation with an smooth potential $V(x)$,

$$-\psi_{xx} + V(x)\psi = E\psi$$

and $E > V_{max}$. The solutions are free particles. Thus the physically interesting quantities are the reflection/transmission coefficients, defined by.

$$\begin{aligned}\psi &\rightarrow T\exp(i\sqrt{(}E)x) \qquad x \rightarrow \infty \\ \psi &\rightarrow \exp(i\sqrt{(}E)x) + R\exp(-i\sqrt{(}E)x) \qquad x \rightarrow -\infty.\end{aligned}$$

In the WKB theory for the Schrödinger equation it is easy to show that the reflection coefficient vanishes to all orders in perturbation theory when $E > V_{max}$ (i.e. there are no turning points.) This does NOT mean, however, that the reflection coefficient is identically zero. The reflection coefficient scales like $\exp(-L/\epsilon)$, which goes to zero faster than any power of ϵ. Since WKB is basically an expansion in powers of ϵ the WKB prediction of the reflection coefficient is zero to all orders in perturbation theory. In other words objects like transmission and reflection coefficients are generally not analytic in ϵ.

In the case of the Schrödinger equation it is well known how to calculate the reflection/transmission coefficient. The method involves looking at the Schrödinger equation in the complex plane, and deforming the path of integration off of the real axis so that it passes through a turning point in the complex plane. The factor of L in the reflection coefficient is basically related to the distance from the real axis to the first complex turning point. Using the known asymptotics of the Airy equation it is then possible to calculate the beyond all orders reflection coefficient[32, 23]. The problem is to do the analogous calculation for the non self-adjoint problem. This seems to be more difficult since the connection problem does not involve the Airy function, which possesses a nice integral representation which makes the connection problem relatively easy, but instead involves a second order Airy-like equation. At this point in time it is not known how to get any sort of quantization condition like we have in the Schrödinger case. At this point we turn to numerics.

4. Numerics

4.1. The Algorithm

In this section we present the results of some numerical experiments on the Zakharov-Shabat eigenvalue problem. The eigenvalue problem was solved using the following numerical method. Beginning with the ZS eigenvalue problem,

$$
\begin{aligned}
i\epsilon v_x &= qw + \lambda v && (4.1)\\
i\epsilon w_x &= \bar{q}v - \lambda w, && (4.2)
\end{aligned}
$$

we integrate the initial value problem for fixed λ and initial conditions

$$
\begin{aligned}
v(-L) &= 1\\
w(-L) &= 0,
\end{aligned}
$$

out to $x = +L$, where L is chosen so that $q(\pm L) \approx 0$. The integration is done with a fourth order Runge-Kutta method. At the righthand boundary $x = +L$ the components of the vector are given by

$$
\begin{aligned}
v(\lambda, x = L) &= v_{right}(\lambda)\\
w(\lambda, x = L) &= w_{right}(\lambda).
\end{aligned}
$$

At this point λ is a free parameter - it is not required to be in the spectrum of the operator. Since $v(\lambda)$ *grows* exponentially in the right half line we are interested in finding zeros of $v_{right}(\lambda)$. In essence we are replacing q with an approximation of large but compact support. If L is chosen to be sufficiently large the error arising from this truncation of the potential is much smaller than other sources of error, such as the error incurred in solving the ODE which defines the function v.

At this point the problem is reduced to that of finding *all* of the zeros of $v(\lambda)$. Conventional methods for finding zeros, such as a Newton scheme, are not attractive for two main reasons. The first reason is the following. Newton type iteration schemes require a good initial guess to be efficient, which is not available in this case. Secondly the function v which we are trying to find the zeros of is quite expensive to calculate - each evaluation of $v(\lambda)$ requires the solution of an ODE! This makes iterative methods, which may require many evaluations of the function, of questionable value.

The algorithm we adopt, which is very similar to the method used in [3, 4], is based on Rouche's theorem. We rectangulate a region of the complex λ plane (Figure 4.1) and numerically calculate the following contour integral,

$$N(\Gamma_{i,j}) = \int_{\Gamma_{i,j}} \frac{v'(\lambda)}{v(\lambda)} d\lambda = Z(\Gamma_{i,j}) - P(\Gamma_{i,j}),$$

where $\Gamma_{i,j}$ is the i, j^{th} rectangle, and Z and P are the number of zeros and poles contained in $\Gamma_{i,j}$. Since $v(\lambda)$ has no poles (v satisfies a linear differential equation with bounded coefficients) the value of this integral is given by $2\pi i n$, the number of zeros of v contained in the rectangle. This, of course, only indicates the presence or absence or a zero. It does not indicate where in the rectangle the zero is located. For this it is useful to calculate the second integral,

$$L(\Gamma_{i,j}) = \frac{1}{N(\Gamma_{i,j})} \int_{\Gamma_{i,j}} \frac{\lambda \frac{dv(\lambda)}{d\lambda}}{v(\lambda)} d\lambda,$$

which has the value z_0, where z_0 is center of mass of the zero contained inside the rectangle. In particular if the contour contains only one zero this integral gives the location. This quantity was found experimentally to be extremely robust. For instance in the worst case scenario, when there is a pole very close (i.e. order of $\Delta\lambda$) to the boundary of the contour then $N(\Gamma)$ has the value

$$N(\Gamma_{i,j}) \approx i\pi + P,$$

where P is a principal value integral. $L(\Gamma_{i,j})$, however, still gives the correct location of the zero. This method was implemented using a fixed rectangulation of the complex plane. A more efficient method would be a "divide and conquer" type approach, which would begin with a rough rectangulation of the complex plane, and would recursively subdivide those rectangles which had a non-zero value for the N integral. However for the range of ϵ covered by these numerics such an approach was not necessary.

The code was tested using exactly solvable potentials (The $\mathrm{sech}(x)$ and square well potentials). In addition for the cases without exact solutions the experiments were repeated increased L and finer discretizations, with essentially no change in the results.

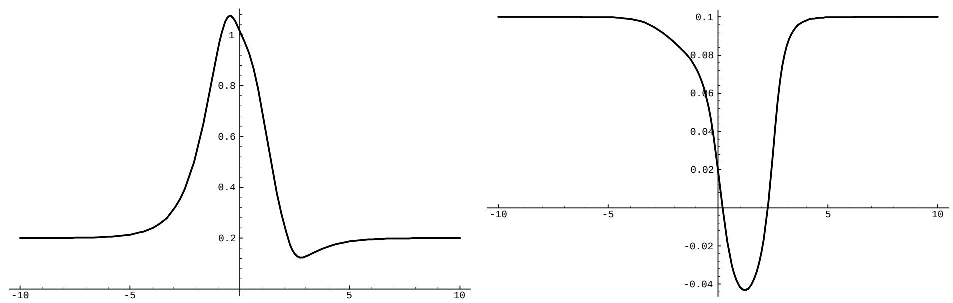

(a) Real Part

(b) Imaginary Part

Figure 3.3: The Phase Function - Homoclinic Case - B

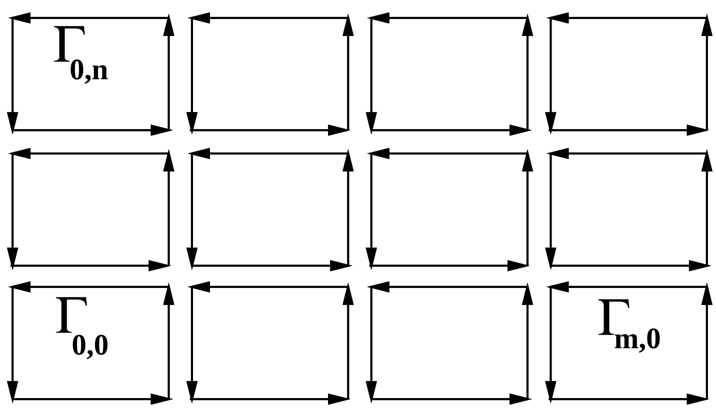

Figure 4.1: Contours for Integrals

In these experiments the relevant region of the complex plane has been subdivided into a $100x100$ grid of rectangles. The contribution of each leg of the rectangle to the contour integral was calculated using 7 grid points per leg. The step size in the Runge-Kutta algorithm varies with ϵ, but typically lies in the range $\Delta x \in [.005, .0025]$.

4.2. A Note On Bounds

The final ingredient in the numerical potion is the question of bounds on the locations of the complex eigenvalues. Obviously we must have some idea of where in the complex plane the eigenvalues are located to have any hope of finding them all. Ideally we would like to have a bound which constrains the eigenvalues to live in a compact region of the complex plane. Unfortunately such a bound is apparently not available. There are two bounds which are of use here. The first, due to Deift[6], guarantees that the ZS eigenvalues live in the shadow of the discriminant curve which arises in the formal WKB theory plus a strip of width ϵ about the real axis. It is this second piece, of course, which is troublesome. It is possible to sharpen this bound somewhat, as is outlined in the appendix. Basically it is possible to show that any eigenvalues with large real parts must have small imaginary parts, so that the region in which the eigenvalues can live, although unbounded, has finite area. So although we cannot be certain that we have found *all* of the eigenvalues we can reasonably hope that the omitted ones, which have small imaginary parts, contribute little to the dynamics.

4.3. The Experiments

4.3.1. Experiment 1

The first experiment is shown in figures 4.3,4.5. The first figure shows the location of the point eigenvalues for several values of ϵ for the potential functions

$$\begin{aligned} S(x) &= \operatorname{sech}(2x) \\ A(x) &= \operatorname{sech}(2x). \end{aligned}$$

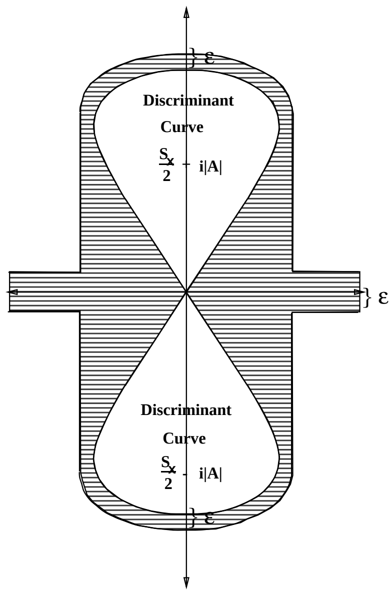

Figure 4.2: Bounds on the Location of Eigenvalues (Deift)

The dotted curve represents the turning point curve Γ. Note that because of the symmetry of the problem only the upper half-plane is shown. The spectrum in the lower half-plane is the mirror image of that in the upper half-plane.

From this experiment it appears that the eigenvalues are approaching some limiting curve, which has a 'Y' shaped appearance. It also appears that the number of eigenvalues scales like $1/\epsilon$, as indicated by the graph and table in figure 4.5.

The third figure (4.6) shows a density plot of the following quantity

$$E_{i,j} = \log |\int_{\Gamma_{i,j}} \frac{f'}{f} d\lambda|.$$

If the numerics were exact this quantity would be $\ln(2\pi)$ if the contour $\Gamma_{i,j}$ contained an eigenvalue and $-\infty$ if the contour did not contain an eigenvalue. The numerically computed integral is, of course, never exactly zero, but away from an eigenvalue the results are quite good. The dark areas correspond to a value of ≈ -20 for $E_{i,j}$, while the light areas to a value of $E \approx \ln(2\pi)$. Thus the error is small away from the actual eigenvalues, and it appears extremely unlikely that the method will produce an eigenvalue where none exists.

The next example shows the spectrum in a degenerate case - one where A and S_x are linearly dependent. In this case the discriminant curve reduces to two line segments and the interior is empty. The particular choice of amplitude and phase in this case is

$$\begin{aligned} S(x) &= \frac{1}{\cosh(2x)} \\ A(x) &= \frac{\sinh(2x)}{\cosh(2x)^2}, \end{aligned}$$

so that $S_x = 2A$, and the discriminant curve reduces to a line segment from $-(1+i)$ to $1+i$, and another from $1-i$ to $-1+i$. It is apparent from the numerics that for non-zero values of ϵ the eigenvalues to not live on the union of these two line segments, and do not appear to approach this curve as $\epsilon \rightarrow 0$. This experiment indicates that the spectrum does not necessarily live inside the turning point curve. The spectrum does, of course, live in the shadow of the turning point curve, as guaranteed by the bound of Deift.

The third experiment shows the spectra in another degenerate case, similar to the one described above. Again we note that the spectra does not live 'inside' the turning point curve, although it does live in the shadow of it. The potential functions for this case are

$$\begin{aligned} S_x &= \frac{1}{\cosh(2x)} - \frac{2x\sinh(2x)}{\cosh^2(2x)} = (\frac{2x}{\cosh(2x)})_x \\ A &= \frac{1}{\cosh(x)}. \end{aligned}$$

This example lacks the even/odd symmetry possessed by the first two experiments, so the spectrum is not right/left symmetric.

The final experiment shows the evolution of the "Y" shaped spectrum from the straight line spectrum which is present in the no phase case. In this experiment the amplitude and phase are given by

$$\begin{aligned} A &= \operatorname{sech}(2x) \\ S &= \mu \operatorname{sech}(2x), \end{aligned}$$

and μ is varied between 0 and .6. When $\mu = 0$ the eigenvalues are purely imaginary. As μ is increased the eigenvalue spacing decreases. At some finite value of μ the first two eigenvalues

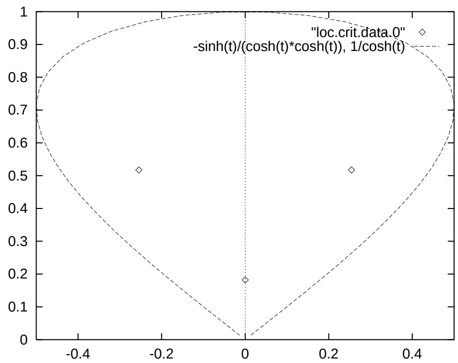

(a) $\epsilon = .2$

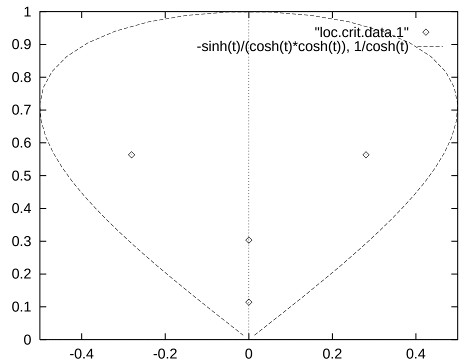

(b) $\epsilon = .159$

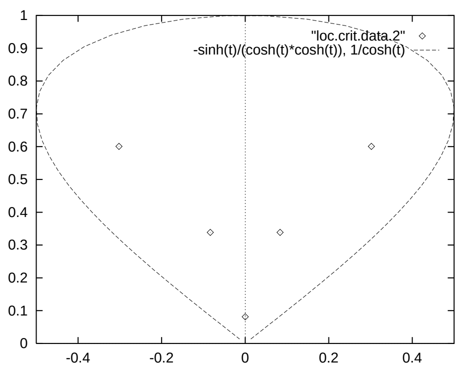

(c) $\epsilon = .126$

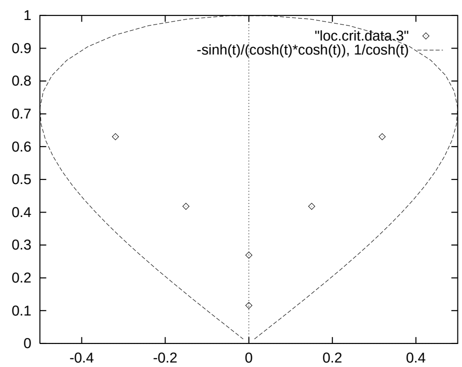

(d) $\epsilon = .1$

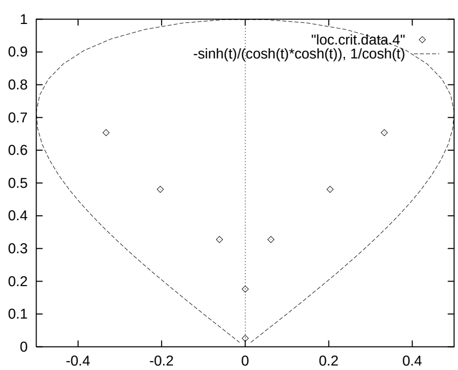

(e) $\epsilon = .0794$

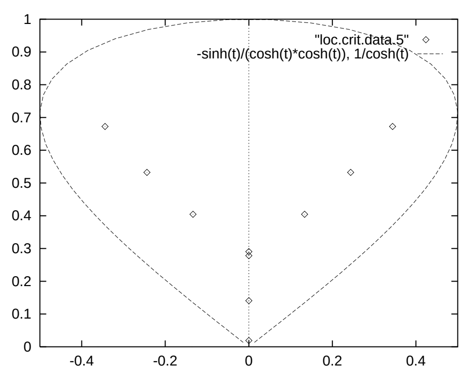

(f) $\epsilon = .0630$

Figure 4.3: Experiment 1: Eigenvalue Locations

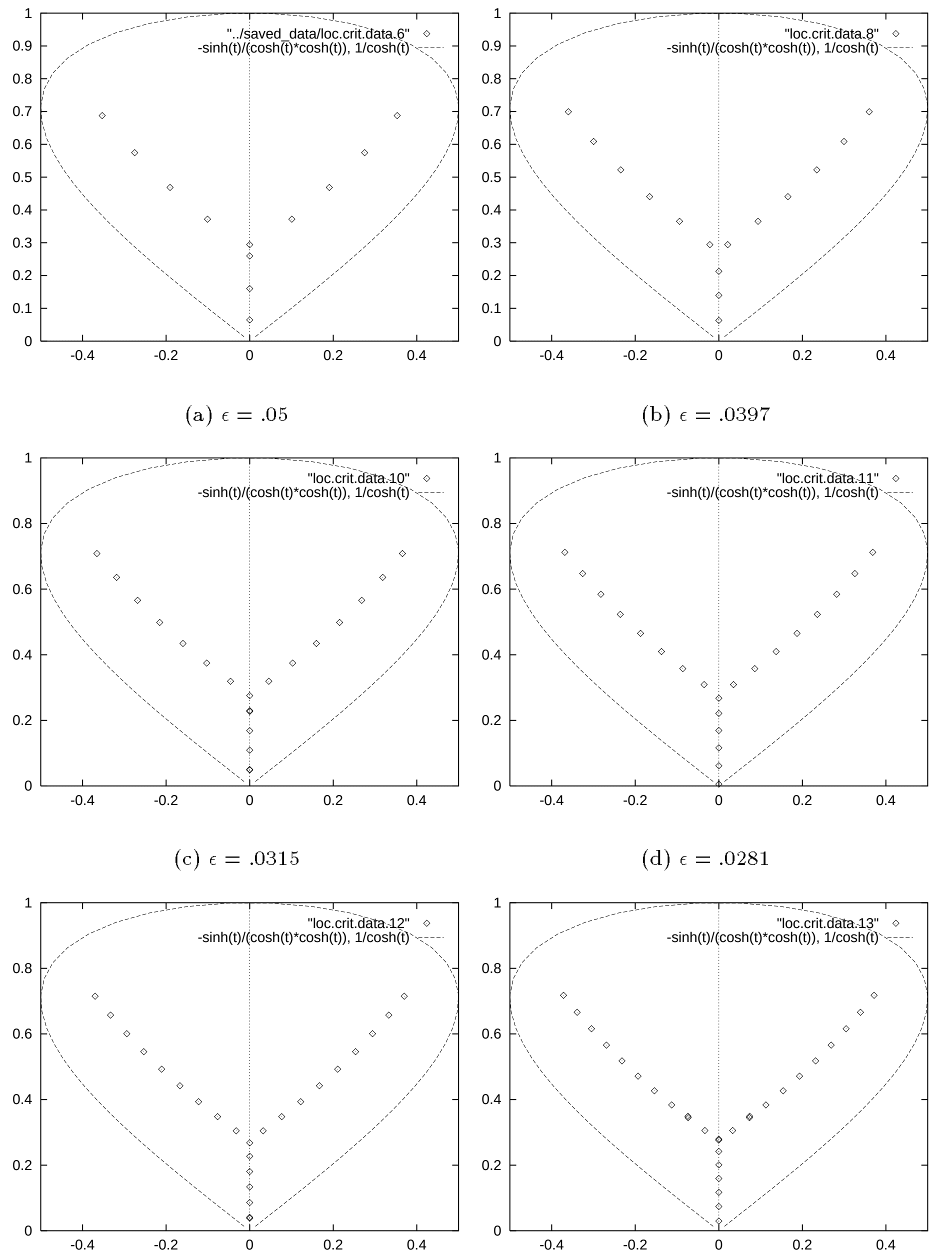

(a) $\epsilon = .05$

(b) $\epsilon = .0397$

(c) $\epsilon = .0315$

(d) $\epsilon = .0281$

(e) $\epsilon = .025$

(f) $\epsilon = .0223$

Figure 4.4: Experiment 1: Eigenvalue Locations (Cont.)

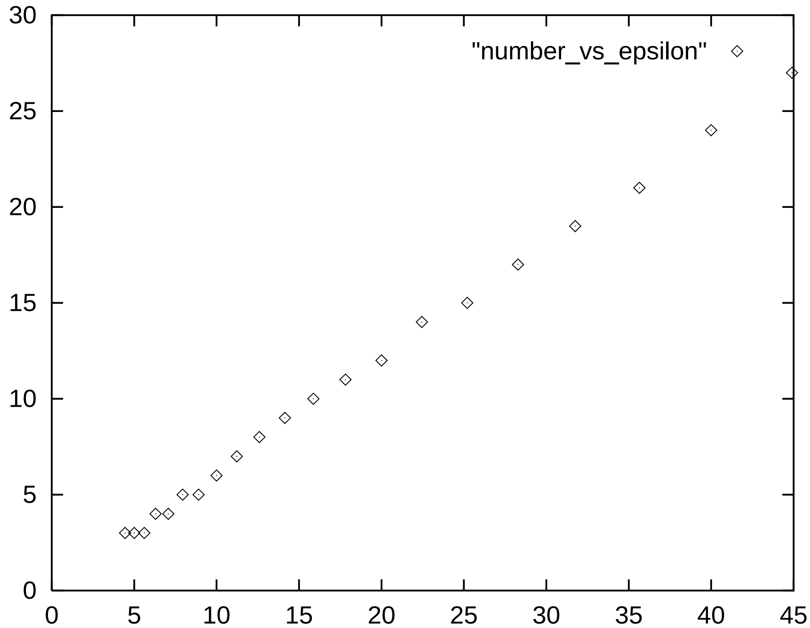

ϵ	ϵ^{-1}	Number	ϵ	ϵ^{-1}	Number
.22449241	4.45	3	.056123112	17.82	11
.20000000	5	3	.050000000	20	12
.17817975	5.61	3	.044544936	22.45	14
.15874011	6.3	4	.039685027	25.2	15
.14142136	7.07	4	.03535534	28.28	17
.12599211	7.94	5	.031498027	31.75	19
.11224621	8.909	5	.028061552	35.64	22
.10000000	10	6	.025	40	24
.089089881	11.225	7	.022272468	44.9	27
.079370053	12.6	8			
.070710688	14.14	9			
.062996053	15.87	10			

Figure 4.5: Experiment 1b: Number of Eigenvalues vs. ϵ^{-1}

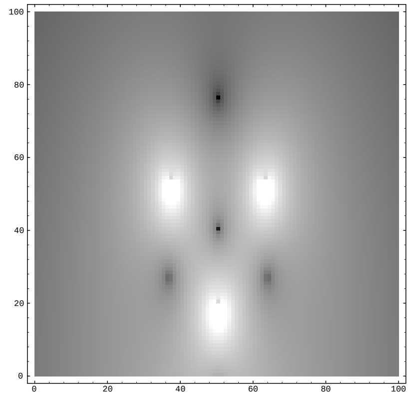

(a) $\epsilon = .2$

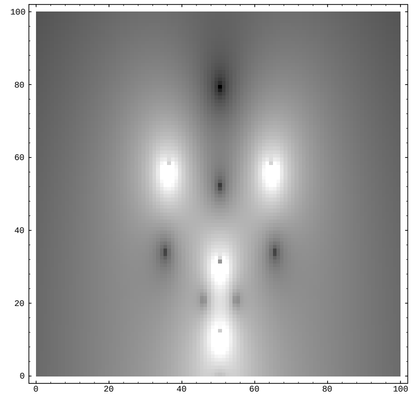

(b) $\epsilon = .159$

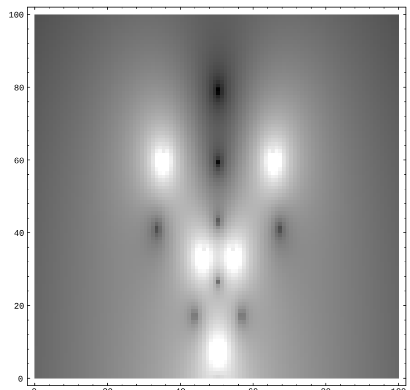

(c) $\epsilon = .126$

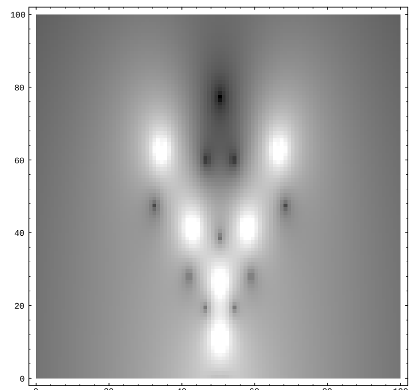

(d) $\epsilon = .1$

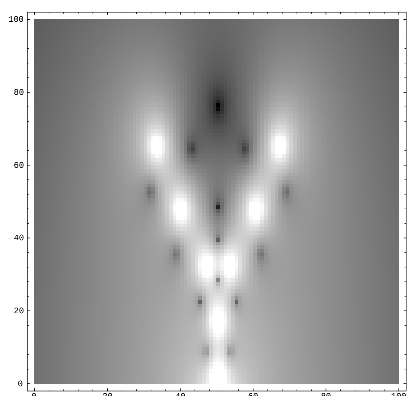

(e) $\epsilon = .0794$

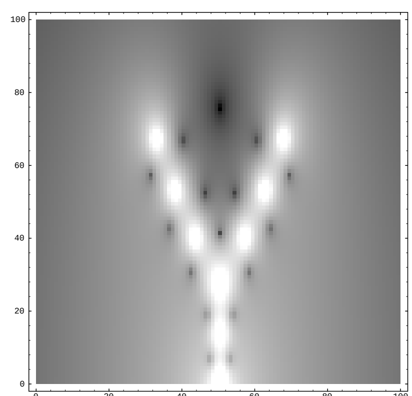

(f) $\epsilon = .0630$

Figure 4.6: Experiment 1c: Density Plot of $Log|\int v'/v d\lambda|$.

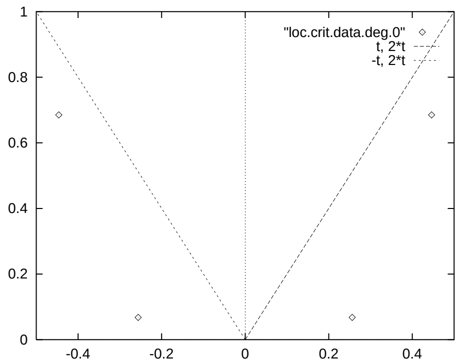

(a) $\epsilon = .2$

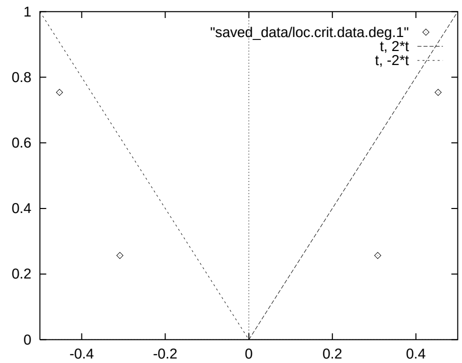

(b) $\epsilon = .159$

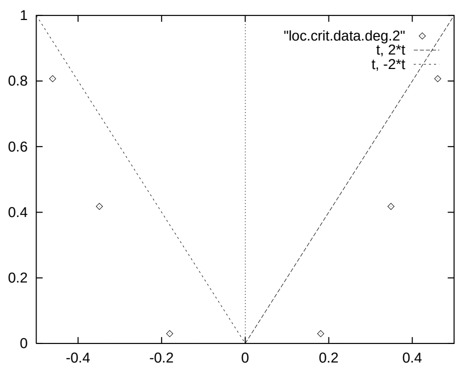

(c) $\epsilon = .126$

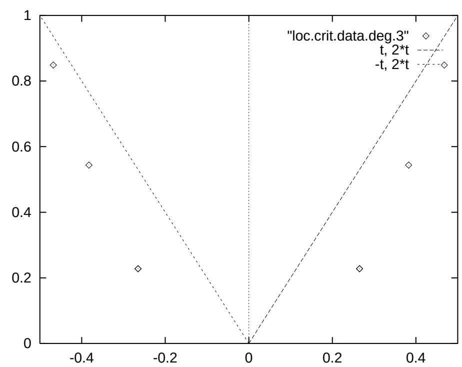

(d) $\epsilon = .1$

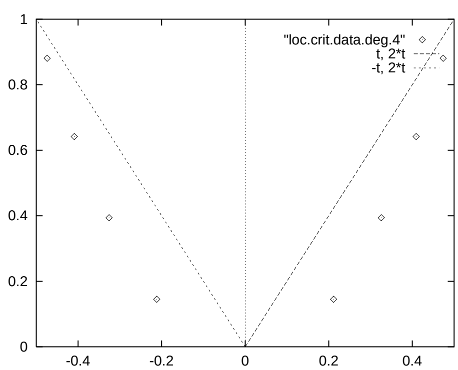

(e) $\epsilon = .0794$

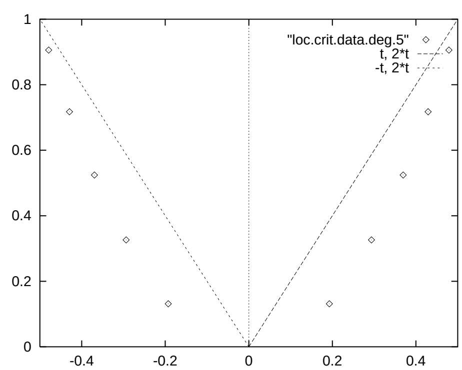

(f) $\epsilon = .0630$

Figure 4.7: Experiment 2: Eigenvalue Locations

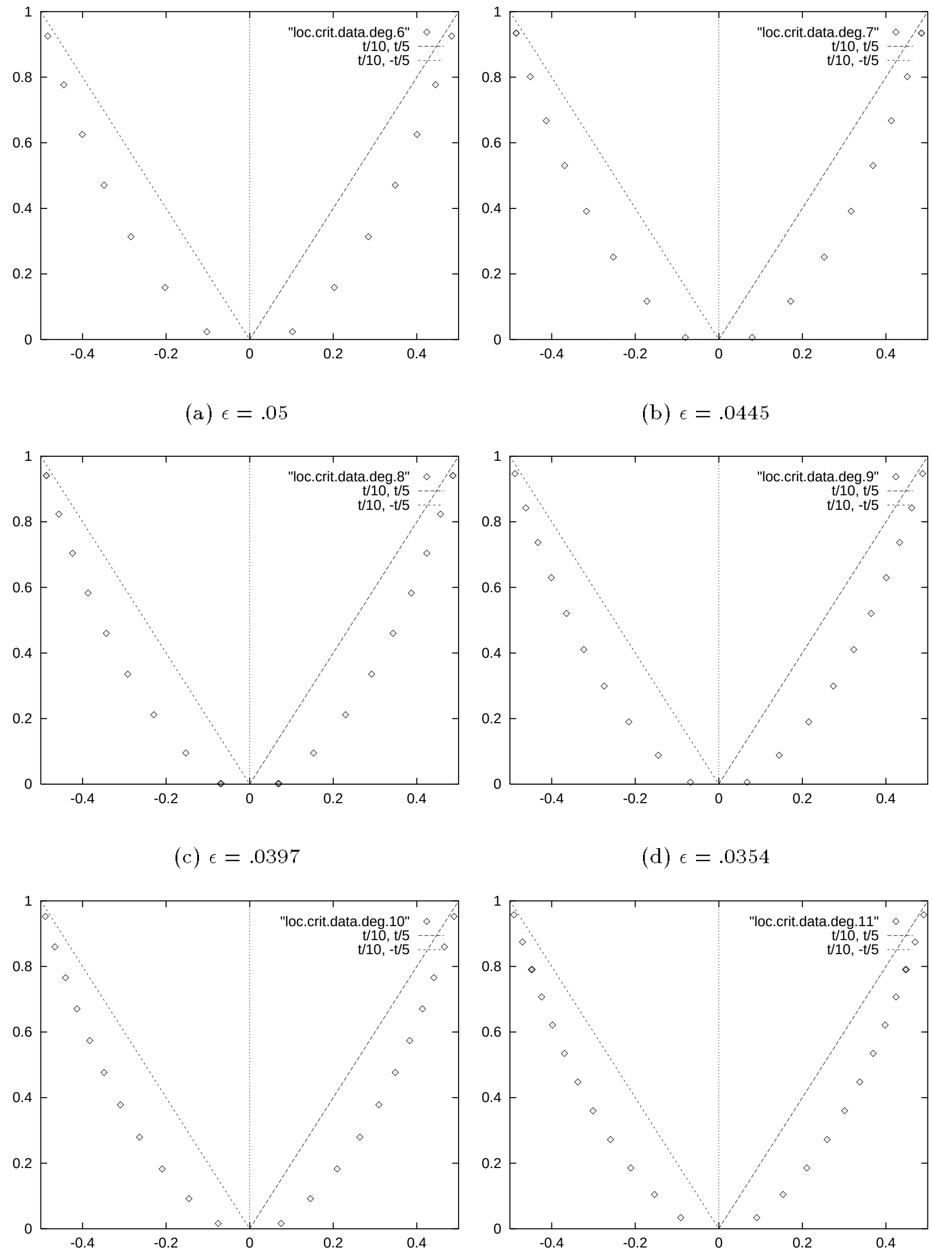

(a) $\epsilon = .05$

(b) $\epsilon = .0445$

(c) $\epsilon = .0397$

(d) $\epsilon = .0354$

(e) $\epsilon = .0315$

(f) $\epsilon = .0281$

Figure 4.8: Experiment 2: Eigenvalue Locations (Cont.)

cross and develop non-trivial imaginary parts. As μ is increased further other eigenvalues cross and the characteristic "Y" shape forms. In the next section we present an asymptotic argument explaining the above observations. Among other things we are able to predict the critical value μ^* where the first pair of eigenvalues crosses.

5. Symmetry Breaking and the Emergence of the 'Y'

In the previous section we saw that for one particular choice of amplitude and phase the spectrum of the Zakharov-Shabat eigenvalue problem approached a 'Y' shaped curve. This curve is generic for what is commonly known as 'shock' initial data - i.e. data where A has a local minima near the origin and S_x has a zero near the origin. It is interesting to try to understand the origin of this curve. In this section we outline an asymptotic argument which is valid for the low energy states (eigenvalues with *large* imaginary parts). In particular this argument predicts a critical value for the phase where a bifurcation from the straight line spectrum associated with the zero phase case to the "Y" shaped spectrum seen in the previous section occurs.

The starting point for the analysis of this phenomenon is the squared eigenvalue problem,

$$\begin{aligned} -\epsilon^2 v_{xx} - |A|^2 v - (\lambda - S_x)^2 v &= i\epsilon A_x v - i\epsilon S_{xx} w \\ -\epsilon^2 w_{xx} - |A|^2 w - (\lambda - S_x)^2 w &= i\epsilon A_x w - i\epsilon S_{xx} v, \end{aligned}$$

which obtained from the standard ZS eigenvalue problem by differentiation and substitution. Neglecting the small right hand side gives the Schrödinger -like eigenvalue problem

$$-\epsilon^2 \psi_{xx} - |A|^2 \psi - (\lambda - S_x)^2 \psi = 0$$

which is satisfied by *both* components of the two-vector (v, w). Clearly for $S_x = 0$ the above squared eigenvalue problem reduces to the Schrödinger eigenvalue problem for the eigenvalue λ^2, with the ground state of the Schrödinger eigenvalue problem, the state with the most negative energy, corresponding to the state with the largest imaginary part.

The idea behind this section is to understand the development of the "Y" shaped spectrum by developing an approximate theory for the near-ground state eigenvalues. Since the lowest eigenfunctions are well-localized spatially it makes sense to expand the potential functions A, S_x

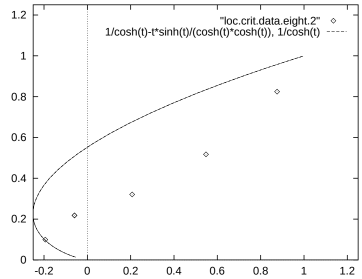

(a) $\epsilon = .126$

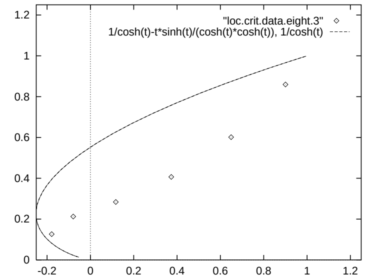

(b) $\epsilon = .1$

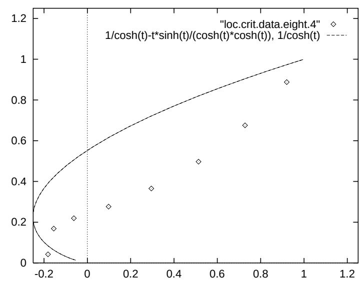

(c) $\epsilon = .0794$

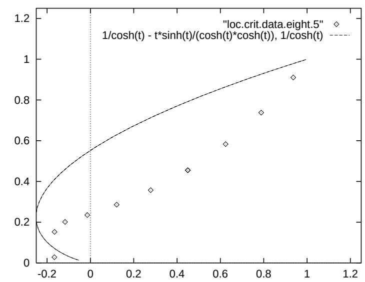

(d) $\epsilon = .0630$

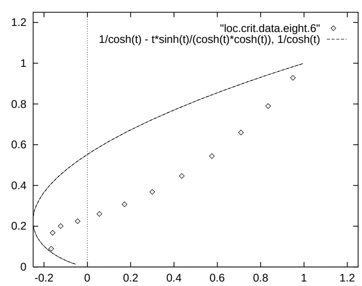

(e) $\epsilon = .05$

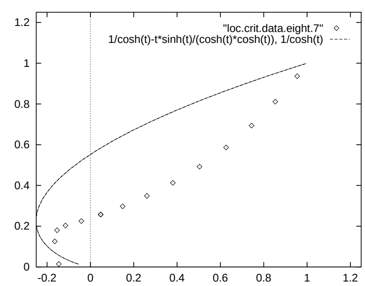

(f) $\epsilon = .0445$

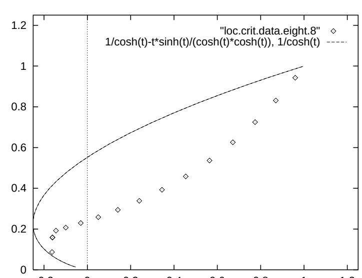

(g) $\epsilon = .0397$

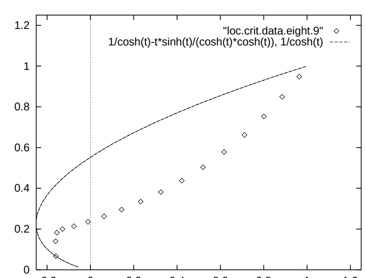

(h) $\epsilon = .0354$

Figure 4.9: Experiment 3: Eigenvalue Locations

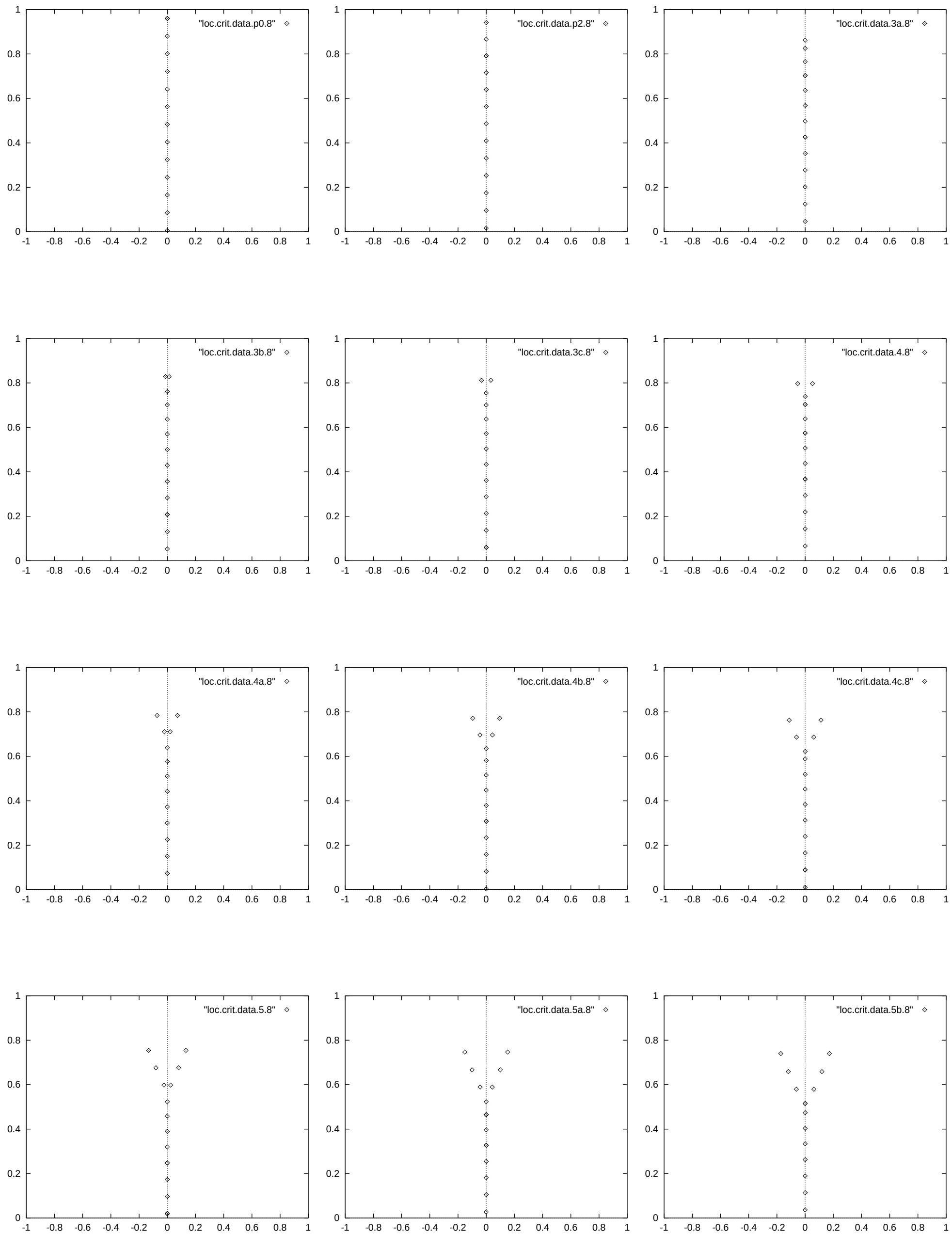

Figure 4.10: Experiment 4: Evolution of the "Y"

locally about critical points. When we do this we get a problem which can be explicitly solved. For S_x small there is a single minima at the origin. Expanding around this point and explicitly solving the resulting equation gives the result that the eigenvalues are purely imaginary, just as in the case when $S_x = 0$. As S_x is increased there is a classical bifurcation - the minima of the effective potential becomes a maxima, and two new minima are born. After this bifurcation takes place the eigenfunctions are no longer localized near the origin, which is a maxima, but are instead localized near the minima of the potential which are located symmetrically about the origin. Since S_x is non-zero near these minima the eigenvalue λ develops a non-zero real part. This is a simple example of the phenomena of symmetry breaking.

Making the substitution $y = x/\epsilon$ and Taylor expanding gives the equation

$$-v_{yy} - (A_0 - \epsilon^2 A_2 y^2)v + (\lambda - \epsilon S_1 y)^2 v = 0,$$

where $A_i = \partial_x^i |A|^2|_{x=0}$ and $S_i = \partial_x^i S|_{x=0}$. Completing the square in y gives the following equation:

$$-v_{yy} - (\alpha\epsilon y + \beta\lambda)^2 v + (\gamma\lambda^2 + A_0)v = 0,$$

where the constants α, β, γ are defined in terms of A_0, A_2, S_1 by the relations

$$\begin{aligned}
\alpha &= \sqrt{A_2 - S_1^2} \\
\beta &= \frac{S_1}{A_2 - S_1^2} \\
\gamma &= \beta^2 - 1 = \frac{A_2}{A_2 - S_1^2}.
\end{aligned}$$

Introducing the new variable $z = y + \frac{\beta\lambda}{\alpha\epsilon}$, which amounts to an energy-dependent shift in the origin, gives the following equation:

$$-v_{zz} - \alpha\epsilon^2 z^2 v + (\gamma\lambda^2 + A_0)v.$$

When $A_2 - S_1^2 > 0$ this is just a standard quantum harmonic oscillator, and the spectrum is completely known. In particular the ground state energy is given by

$$\lambda_{ground}^2 = -\frac{\alpha}{A_2}(A_0 - 1/2\epsilon)$$
$$\lambda_{ground} = \pm i\gamma^{-1/2}(A_0 - 1/2\epsilon)^{1/2}$$

Notice a few things about this approximation. The shift in origin, $\frac{\beta\lambda}{\alpha\epsilon}$, is purely imaginary. This means that we expect the real zeros of the harmonic oscillator wavefunctions to move off of the axis. It is also apparent that since $\gamma > 1$ the effect of turning on the phase is to decrease the spacing between eigenvalues, and to increase the energy of the ground state. These observations will be confirmed later in this section by numerical experiment.

It is clear that this approximation is expected to be valid for small quantum numbers, when the eigenfunctions are well localized and the Taylor expansion of the potential is justified. It is also clear that this expansion should be valid when $A_2 - S_1^2 >> 0$, so that higher order terms in the potential can be dropped.

When $A_2 - S_1^2 < 0$ the origin is no longer a local minima of the effective potential $A^2 + S_x^2$, but is instead a local maxima. In this case the eigenfunctions will not be supported near the origin, but instead will be supported near the new local minima which are born to either side of the origin. The same calculation done above can be repeated in this case, expanding the potential about x^*, the minima of $A^2 + S_x^2$, rather than the origin. Since $S_x(x^*) \neq 0$ the eigenvalue λ develops a non-trivial real part. This real part will be positive for the minima on the right half-line and negative for the minima on the left half-line. This is the source of the "Y" shaped spectrum.

If we consider the specific case $A = \operatorname{sech}(2x), S_x = \mu \operatorname{sech}(2x)$ the above theory predicts the emergence of the "Y" shaped curve (the collision and subsequent splitting of the ground state and first excited eigenvalue) at the critical value $\mu^* = 2^{-3/2} + o(1) \approx .3536 + o(1)$. Figure 5 shows a plot of the numerically calculated value of $\mu^*(\epsilon)$ vs. ϵ. The errorbars in the graph represent the fact that there is a range of values of μ where the program is unable to resolve the individual eigenvalues, but rather reports a double eigenvalue. A numerical fit to the data points gives $\mu(0) \approx .36$, in good agreement with the predicted value of $2^{-3/2}$.

The next picture shows the numerically calculated eigenfunctions. The eigenfunctions were calculated in the following way. The spectrum was calculated using the contour integral method outlined earlier. Once the eigenvalues were determined this information was used in a standard shooting method to numerically calculate the eigenfunctions. The potential was chosen to be $A = S = \operatorname{sech}(2x)$, corresponding to $\mu = 1$. Since $\mu = 1$ is much bigger than the critical

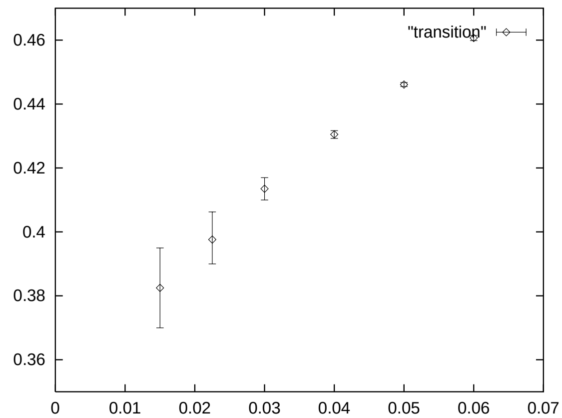

value $\mu^* = 2^{-3/2}$ the eigenfunctions are expected to break symmetry. Indeed this is exactly what we find. Figure 5 shows the eigenfunctions ordered according to decreasing imaginary parts. The first two graphs show the amplitudes of the v and w components of the eigenvectors with the largest imaginary parts. The solid line is the v component, while the dotted line is the w component. As argued earlier the eigenfunction corresponding to the eigenvalue with a positive real part is strongly biased to the right, while the eigenfunction corresponding to the eigenvalue with a negative real part is strongly biased to the left. Also show are some higher energy eigenfunctions. It is obvious that the bias is still present, but less pronounced than in the ground state case. The final picture shows the eigenfunction corresponding to an eigenvalue have no real part - part of the 'stem' of the "Y". This eigenfunction does not break symmetry. This is because symmetry breaking is a 'low energy' phenomenon. High enough energy states always preserve symmetry.

6. Conclusions

We have seen in this paper that the spectrum of the non self-adjoint ZS eigenvalue problem appears quite well behaved. For typical analytic, L_2 potentials the number of eigenvalues seems to scale like ϵ^{-1}, and the eigenvalues appear to approach some limiting distribution which is supported on a curve as $\epsilon \to 0$. A complete understanding of these observations is currently

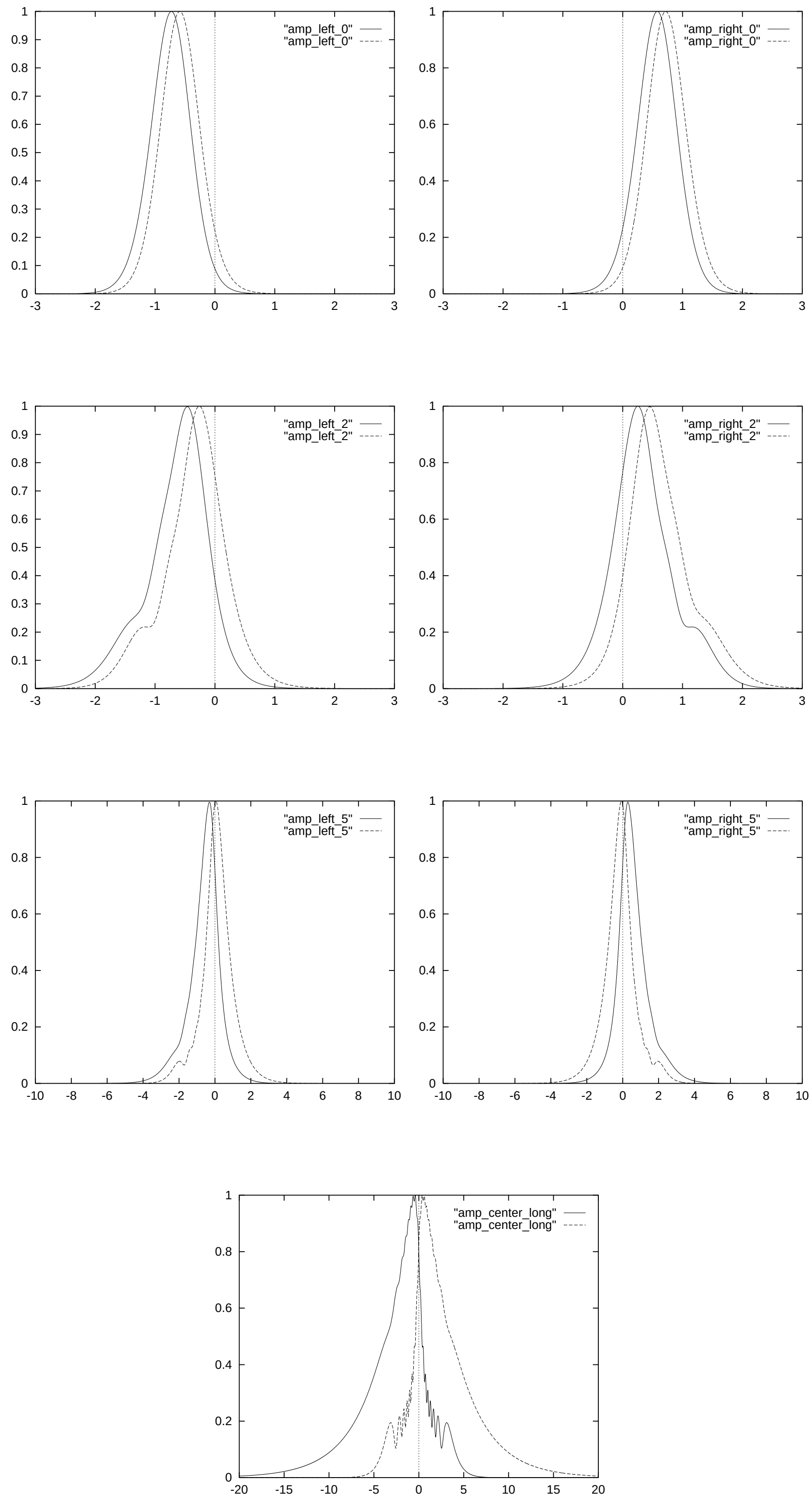
"amp_left_0"
"amp_left_0"
"amp_right_0"
"amp_right_0"
"amp_left_2"
"amp_left_2"
"amp_right_2"
"amp_right_2"
"amp_left_5"
"amp_left_5"
"amp_right_5"
"amp_right_5"
"amp_center_long"
"amp_center_long"

lacking, but in each case we can give a partial result. A partial understanding of the scaling of the number of eigenvalues vs. epsilon follows trivially in the case of reflectionless potentials from the well known trace formula for the ZS eigenvalue problem. Specifically

Lemma 6.1: *Suppose q is a reflectionless potential with fixed L_2 norm. Let $N_\alpha(\epsilon)$ be the number of eigenvalues with $|\lambda_{\mathcal{I}m}| \geq \alpha$. Then $N_\alpha(\epsilon) \leq \frac{1}{\alpha\epsilon}$.*

Proof *Follows trivially from the trace formula*

$$\begin{aligned} \epsilon^{-1}||q||^2 &= \sum_{\{\lambda|\lambda_{\mathcal{I}m}>0\}} \lambda_{\mathcal{I}m} \\ &\geq \sum_{\lambda|\lambda_{\mathcal{I}m}>\alpha} \alpha = \alpha N_\alpha(\epsilon). \end{aligned}$$

So in the case of reflectionless potentials if there are any 'extra' eigenvalues above the $O(\epsilon^{-1})$ present in the self adjoint (or constant phase) case they must collect near the real axis. The necessity of excluding eigenvalues with small imaginary parts is, quite obviously, built in to this simple proof. Any argument bounding the number without such a restriction would have to be based on a much more sophisticated argument.

It is interesting that in the attempting to bound the locations of the eigenvalues and in attempting to bound the number we are thwarted by the possibility of having many eigenvalues with small imaginary parts. It seems to suggest that this is a real possibility, and not simply a defect in the method of proof. The intuitive picture is that these eigenvalues could arise from "resonances" crossing the branch cut along the real axis and becoming proper eigenvalues. Indeed the heuristic arguments which have been put forth suggesting that the number of eigenvalues scales as ϵ^{-2} have been based on the existence of resonances on the real axis. While the argument mentioned above and the numerical results both suggest that the proper scaling is $N(\epsilon) \propto \epsilon^{-1}$ it should be stressed that all of the numerics have, of course, been done on a finite domain, and there is still a real possibility of a large or even and infinite number of eigenvalues located close to the real axis. Indeed eigenvalues located very close to the real axis would be quite difficult to detect due to the change in the boundary condition which occurs across the real axis. On the other hand we should reiterate out belief, or rather our hope, that the existence of eigenvalues with small imaginary parts should not be too important to the NLS dynamics.

The "Y" shaped curve on which the eigenvalues lie for 'shock' initial data can, as we have seen, be understood simply in terms of a simple symmetry breaking problem. While this argument does not tell us the exact shape of the curve it does allow us to make predictions about quantities such as the critical phase necessary for the onset of the bifurcation, the eigenvalue spacing, the ground state energy, etc. While it would be interesting to derive the exact shape of this "Y" we are still able to get much interesting information from this simple argument. What we lack, unfortunately, is information on quantities such as norming constants which are necessary for doing the inverse problem.

Finally it should be mentioned that in numerical simulations of a discrete non self-adjoint eigenvalue problem related to the Toda lattice K. McLaughlin[27] has observed "Y" shaped spectra which are strikingly similar to those we have observed for the ZS eigenvalue problem. This suggests that the results here are not specific to the ZS scattering problem, but rather have analogs for some class of non selfadjoint problems.

Acknowledgement: I would like to thank David Levermore and Ken McLaughlin for interesting and useful conversations and Percy Deift for his extensive help and encouragement.

6.1. Appendix

In this section we prove that any complex eigenvalues of the ZS eigenvalue problem must satisfy the inequalities

$$|\lambda_{\mathcal{I}m}| \leq C_1 |\lambda_{\mathcal{R}e}|^{-1}$$

and

$$|\lambda_{\mathcal{I}m}| \leq C_2 |\lambda_{\mathcal{R}e}|^{-2}.$$

This guarantees that any eigenvalues with large real part must lie very close to the real axis. It is hoped that these eigenvalues, since they correspond to solitons with very small mass, are in some sense unimportant in the dynamics of focusing NLS. The idea behind the proof is simple - it consists of taking powers of the eigenvalue problem and bounding the real and imaginary parts by simple inequalities. The eigenvalue problem is given by

$$\begin{aligned} i\epsilon v_x + qw &= \lambda v \\ i\epsilon w_x + \bar{q}v &= -\lambda w. \end{aligned}$$

Multiplying the first equation by $\bar{v}$ and integrating gives

$$2\lambda_{\mathcal{I}m} \int |v|^2 = \int qw\bar{v} - \bar{q}\bar{w}v.$$

Similarly the second equation gives

$$2\lambda_{\mathcal{I}m} \int |w|^2 = \int qw\bar{v} - \bar{q}\bar{w}v.$$

This allows us to conclude that for strictly complex eigenvalues ($\lambda_{\mathcal{I}m} \neq 0$) the two components v, w have the same L_2 norm. From this point on we will assume that $||v||^2 = ||w||^2 = 1$. Using this fact in either of the above equations, along with the Cauchy-Schwartz inequality, gives

$$|\lambda_{\mathcal{I}m}| \leq ||q||_\infty.$$

Next notice that by adding the complex conjugates instead of subtracting we get the following identity for the real part of λ :

$$\lambda_{\mathcal{R}e} = \int i\epsilon(\bar{v}v_x - \bar{v}_x v + \bar{w}_x x - \bar{w}w_x).$$

Multiplying the v equation by $\bar{v}_x$ and integrating gives

$$2\lambda_{\mathcal{R}e}\lambda_{\mathcal{I}m} = \int \bar{v}wq_x + v\bar{w}\bar{q}_x$$

which immediately yields

$$|\lambda_{\mathcal{I}m} \leq \frac{\epsilon||q_x||_\infty}{|\lambda_{\mathcal{R}e}|}.$$

Squaring the eigenvalue problem leads to the following eigenvalue problem for λ^2.

$$\begin{pmatrix} -\partial_{xx} - |q|^2 & iq_x \\ i\bar{q}_x & -\partial_{xx} - |q|^2 \end{pmatrix} \begin{pmatrix} v \\ w \end{pmatrix} = \lambda^2 \begin{pmatrix} v \\ w \end{pmatrix}.$$

Multiplying the v equation by $\bar{v}_x$ and the w equation by $\bar{w}_x$ yields the following equality

$$\lambda_{\mathcal{I}m}\lambda_{\mathcal{R}e}^2 = \epsilon \int (|v|^2 - |w|^2)(|q|^2)_x + \int i\epsilon^2 q_{xx}\bar{v}w - i\bar{q}_{xx}v\bar{w},$$

or

$$\lambda_{\mathcal{I}m} \leq \frac{C''}{\lambda_{\mathcal{R}e}^2}$$

where $C'' = \epsilon^2||q_{xx}||_\infty + \epsilon|||q|_x^2||_\infty$. It is clear that many more such identities and corresponding inequalities can be derived.

References

[1] T. Ya. Azizov and I. S. Iokhvidov. *Linear Operators in Spaces with an Indefinite Metric.* Wiley-Interscience, 1989.

[2] M.V. Berry. Semiclassically Weak Reflections above Analytic and Nonanalytic Potential Barriers. *J. Phys. A: Math. Gen.*, 15:3693–3704, 1982.

[3] A.R. Bishop, M.G. Forest, D.W. McLaughlin, and E. A. Overman II. A Quasi-periodic Route to Chaos in a Near Integrable PDE. *Physica D.*, 23:293, 1986.

[4] A.R. Bishop, D.W. McLaughlin, and E. A. Overman II. Coherence and chaos in the driven damped sine gordon equation. *Physica D.*, 19, 1986.

[5] J.C. Bronski and D.W. McLaughlin. Semiclassical Behavior in the NLS equation: Optical Shocks and Focusing Instabilities. In *Singular Limits of Dispersive Waves*, 1994.

[6] P. Deift. Personal Communications.

[7] P. Deift and X. Zhou. A Steepest Descent Method for Oscillatory Riemann-Hilbert Problems: Asymptotics for the MKdV Equation. *Annals of Math.*, 137:295–368, 1993.

[8] P. Deift and X. Zhou. Long-time Asymptotics for the Autocorrelation Function of the Transverse Ising Chain at the Critical Magnetic Field. In *Singular Limits of Dispersive Waves*, 1994.

[9] Ercolani, Serre, and Levermore, editors. *Singular Limits of Dispersive Waves*, volume 320 of *NATO/ASI B: Physics*, New York, 1994. NATO, Plenum Press.

[10] N. Ercolani, S. Jin, C.D. Levermore, and W.D.McEvoy. The Zero Dispersion Limit of the NLS/mKdV Hierarchy for the Nonselfadjoint ZS Operator. *Preprint*, 1993.

[11] H. Flashka, M.G. Forest, and D.W. McLaughlin. Multiphase Averaging and the Inverse Spectral Solutions of the KdV Equation. *Comm. Pure. Appl. Math*, 33:739–784, 1980.

[12] M. G. Forest and J.E. Lee. Geometry and Modulation Theory for Periodic Nonlinear Schrodinger Equations. In *Oscillation Theory, Computation, and Methods of Compensated Compactness*, IMA Volumes on Mathematics and its Applications, pages 35–69, 1986.

[13] C.S. Gardner, J.M. Greene, M.D. Kruskal, and R.M. Miura. Method for Solving the Korteweg-de Vries Equation. *Phys. Rev. Lett.*, 19:1095–1097, 1967.

[14] V.V. Geogjaev. The Quasiclassical Limit of the Inverse Scattering Method. In *Singular Limits of Dispersive Waves*, 1994.

[15] J. Gibbons and Y. Kodama. Solving Dispersionless Lax Equations. In *Singular Limits of Dispersive Waves*, 1994.

[16] A.K. Hobbs, W.L. Kath, and G.A. Kriegsman. Bending Losses in Optical Fibers. In *Asymptotics Beyond All Orders*, 1991.

[17] S. Jin. *The Semiclassical Limit of the Defocusing Nonlinear Schrodinger Flows*. PhD thesis, University of Arizona, 1990.

[18] S. Jin, C.D. Levermore, and D.W. McLaughlin. The Behavior of the NLS Equation in the Semiclassical Limit. In *Singular Limits of Dispersive Waves*, 1994.

[19] S. Kamvissis. Critical and Subcritical Cases of the Toda Shock Problem. In *Singular Limits of Dispersive Waves*, 1994.

[20] R.E. Langer. On The Asymptotic Solution of Ordinary Differential Equations. *Trans. Amer. Math. Soc.*, 33(23), 1931.

[21] P. Lax and C.D. Levermore. The Small Dispersion Limit of the KdV Equation I,II,II. *Comm. Pure Appl. Math.*, 36:253–290,571–593,809–829, 1983.

[22] C.D. Levermore. The Hyperbolic Nature of the Zero Dispersion KdV Limit. *Comm. P.D.E.*, 13(4):495–514, 1988.

[23] Levine, Segur, and Tanveer, editors. *Asymptotics Beyond All Orders*, volume 284 of *NATO/ASI B: Physics*, New York, 1991. NATO, Plenum Press.

[24] B. Levitan and Sargsjan. *Sturm-Liouville and Dirac Operators*. MIA. Kluwer Academic Publishers, 1989.

[25] Z.V. Lewis. Semiclassical Solutions of the Zakharov Shabat Scattering Problem for Phase Modulated Potentials. *Physics Letters A*, 112(3/4), 1985.

[26] D.W. McLaughlin and E. A. Overman II. Whiskered Tori for Integrable Pde's; Chaotic Behavior in Near Integrable Pde's. *Surveys in Applied Math.*, To Appear.

[27] K. McLaughlin. Personal Communications.

[28] K. McLaughlin. *A Continuum Limit of the Toda Lattice*. PhD thesis, New York University - Courant Institute, 1994.

[29] R.E. Meyer. Quasiclassical Scattering Above Barriers in One Dimension. *Journal of Mathematical Physics*, 17(6), 1976.

[30] R.E. Meyer. Exponential Asymptotics. *SIAM Review*, 22(2):213–223, 1980.

[31] R.E. Meyer. Exponential Asymptotics for Partial Differential Equations. In *Asymptotics Beyond All Orders*, 1991.

[32] V.L. Pokrovskii and I.M. Khalatnikov. On the Problem of Above-Barrier Reflection of High Energy Particles. *Soviet Physics JETP*, 13(6):1207–1210, 1961.

[33] F. Schwabl. *Quantum Mechanics.* Springer Verlag, 1992.

[34] F.R. Tian. On the Initial Value Problem of the Whitham Averaged System. In *Singular Limits of Dispersive Waves*, 1994.

[35] S. Venakides. The Generation of Modulated Wavetrains in the Solution of the KdV Equation. *Comm. Pure Appl. Math.*, 38:883–909, 1985.

[36] S. Venakides. The Zero Dispersion Limit of the KdV Equation with Periodic Initial Data. *AMS Trans.*, 301:189–225, 1987.

[37] S. Venakides. Higher Order Lax-Levermore Theory. *Comm. Pure Appl. Math.*, 43:335–362, 1990.

[38] W. Wasow. *Linear Turning Point Theory.* Springer Verlag, 1985.

[39] G.B. Whitham. *Linear and Nonlinear Waves.* Wiley, New York, 1974.

[40] O.C. Wright. Explicit Construction of the Lax-Levermore Minimizer for the KdV Zero Dispersion Limit. In *Singular Limits of Dispersive Waves*, 1994.

[41] V.E. Zakharov and A.B. Shabat. Exact Theory of Two-Dimensional Self-Focusing and One-Dimensional Self-Modulation of Waves in Nonlinear Media. *Sov. Phys. JETP*, 34:62–69, 1973.

[42] V.E. Zakharov and A.B. Shabat. Interaction Between Solitons in a Stable Medium. *Sov. Phys. JETP*, 37:823–828, 1973.